Supporting Information

Incorporation of CeO_2 with Ni-Co mixed metal phosphide boosts electrochemical seawater oxidation performance

Bin Fang,[a,b,c,d] *Xiang Chu,*[c,d] *Xiaoxiao Han,*[c,d] *Jianning He,*[c,d] *Baokang Geng,*[c,d] *Lingxi jia,*[c,d] *Xiao Wang,*[c,d,*] *Shuyan Song*[c,d,*] *and Hongjie Zhang*[c,d,e,*]

[a] School of Rare Earths, University of Science and Technology of China, Hefei 230026, China

[b] Ganjiang Innovation Academy, Chinese Academy of Sciences, Ganzhou 341000, China

[c] State Key Laboratory of Rare Earth Resource Utilization, Changchun Institute of Applied Chemistry, Chinese Academy of Sciences, Changchun 130022, China

[d] School of Applied Chemistry and Engineering, University of Science and Technology of China, Hefei 230026, China

[e] Department of Chemistry, Tsinghua University, Beijing 100084, China

*Email: wangxiao@ciac.ac.cn; songsy@ciac.ac.cn; hongjie@ciac.ac.cn

Experimental Section

Chemicals.

p-Phthalic acid ($C_8H_6O_4$, BDC) and Cerium nitrate hexahydrate [$Ce(NO_3)_3·6H_2O$] were purchased from Aladdin Chemical Co., Ltd. Ethyl alcohol (C_2H_5OH), isopropyl alcohol(C_3H_8O) and potassium hydroxide (KOH) were acquired from Tianjin Beilian Fine Chemical Co., Ltd. N,N-Dimethylacetamide (C_4H_9NO, DMAC) was purchased from Tianjin Fuyu Fine Chemical Co., Ltd. Cobalt nitrate hexahydrate [$Co(NO_3)_2·6H_2O$] and sodium hypophosphite (NaH_2PO_2) were obtained from Shanghai Macklin Biochemical Co., Ltd. Nickel nitrate hexahydrate [$Ni(NO_3)_2·6H_2O$] and sodium chloride (NaCl) were purchased from XiLong Scientfic Co., Ltd. Seawater was taken from the Huanghai Sea in Qingdao, China. All chemicals were analytical grade and used without further purification.

Preparation of NiCo-MOF and CeO_2-NiCo-MOF.

Typically, $Co(NO_3)_2·6H_2O$ (0.1 mM), $Ni(NO_3)_2·6H_2O$ (0.2 mM) and $Ce(NO_3)_3·6H_2O$ (0.018 mM) were dissolved in 10 mL DMAC with stirring for 30 min. Then, the above solution was mixed with a DMAC solution (5 mL) of BDC (0.1 mM) followed by adding 9 mL isopropyl alcohol. Afterwards, the mixture was transferred into 50 mL Teflon autoclave and heated at 150 °C for 3 h. After cooling down to room temperature, the product was washed by deionized water and ethanol three times. Finally, the solid powder was dried at 60 °C overnight, this obtained product was named CeO2-NiCo-MOF. The preparation procedure of NiCo-MOF is the same as above, except that $Ce(NO_3)_3·6H_2O$ is not added.

Preparation of CeO_2-$Co_{2-x}Ni_xP$@C and $Co_{2-x}Ni_xP$@C.

The preparation of CeO_2-$Co_{2-x}Ni_xP$@C involves two steps, direct annealing and phosphorization treatment. In the first step, the as-obtained CeO_2-NiCo-MOF was heated at 300 °C for 3 h in air and the heating rate is 5 °C min^{-1}. After cooling down to room temperature, the obtained black product was CeO_2-$CoNiO_x$@C. In the next phosphorization procedure, 10 mg CeO_2-$CoNiO_x$@C and 200 mg NaH_2PO_2 were placed on both sides in a quartz boat, and the NaH_2PO_2 was located on the upstream side of the furnace. Then, the boat was calcined at 300 °C for 2 h with a heating rate of 2 °C min^{-1} under N_2 flow. After cooling down to room temperature naturally, the product of CeO_2-$Co_{2-x}Ni_xP$@C was obtained. The preparation of $Co_{2-x}Ni_xP$@C is the same as above, except that the raw material was NiCo-MOF.

Characterization.

Field emission scanning electron microscope (FEI, Qunta250, USA) and transmission electron microscope (FEI, TECNAI G2) accelerating voltage of 20 kV were employed to characterize the morphologies of all samples. Bruker D8 Focus powder X-ray diffractometer with Cu-Kα radiation (λ = 1.5418 Å) was used to determine the XRD pattern. Determination of element content was carried out using inductively coupled plasma optical emission spectroscopy (ICP-OES) with model Varian Liberty 200. X-ray photoelectron spectroscopy (XPS) analyses were performed by ESCALAB-MKII 250 photoelectron spectrometer with Kα radiation. CHI 660E electrochemistry workstation (CH Instruments, Inc., Shanghai) was used to carry out electrochemical tests.

Electrochemical measurements.

Electrochemical measurements were conducted using CHI 660E electrochemistry workstation with a standard three-electrode system. The working electrode was the carbon paper coated with catalysts, an Ag/AgCl (saturated 3 M KCl electrolyte) was used as reference electrode and the counter electrode was a platinum foil. All linear sweep voltammograms (LSVs) were measured at a scan rate of 5 mV s^{-1}. All potentials were calibrated to the reversible hydrogen electrode (RHE) using the Nernst equation: $E_{RHE} = E_{Ag/AgCl} + 0.059\ pH + 0.197$. The fresh electrolyte was purged with N_2 for 30 min before tests. The electrochemical double-layer capacitance (C_{dl}) was measured from the CV curves from the double-layer region in the potential range of 0.1 and 0.2 V *vs.* RHE with different scan rates and it was calculated according to the following formula:

$$C_{dl} = \frac{Ja - Jc}{v}$$

in which C_{dl} is the double-layer capacitance, Ja represents the positive scan current at 0.15 V vs. RHE, Jc represents the negative scan current at 0.15 V vs. RHE and v is the scan rate.[24] The ECSA values were calculated using the following equation：

$$ECSA = \frac{Cdl}{Cs}$$

in which C_{dl} is the double-layer capacitance, C_s is the specific capacitance, and in this study, the value is estimated to be 40 μF cm^{-2} according to the reported literature.[25]

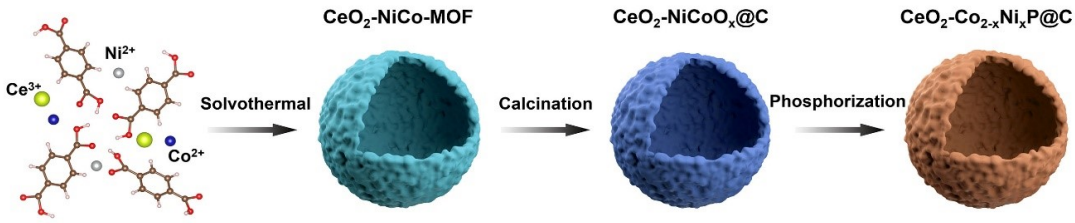

Figure S1. Schematic illustration for the preparation of the CeO_2-$Co_{2-x}Ni_xP$@C catalyst.

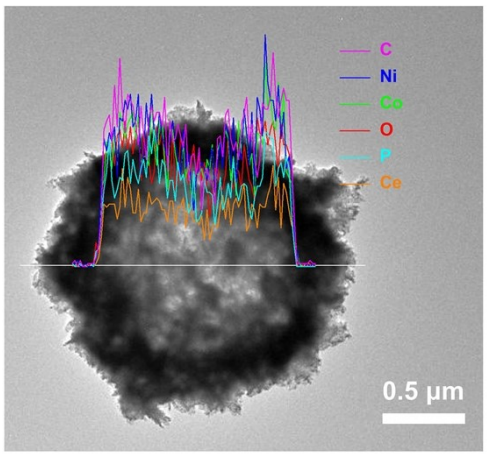

Figure S2. STEM-EDX line profile of CeO_2-$Co_{2-x}Ni_xP$@C.

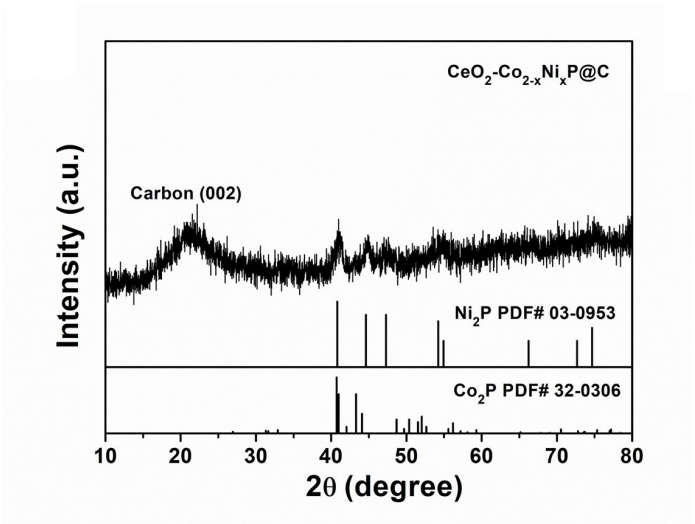

Figure S3. XRD pattern of the as-prepared CeO_2-$Co_{2-x}Ni_xP$@C.

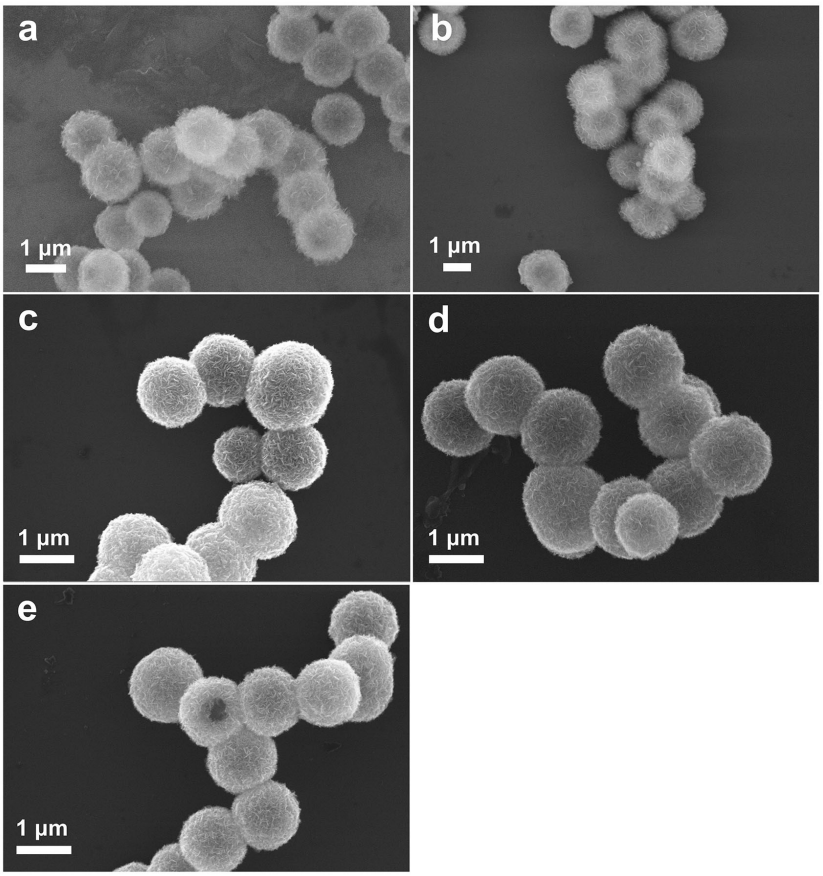

Figure S4. SEM images of (a) NiCo-MOF, (b) CeO_2-NiCo-MOF, (c) $NiCoO_x$@C, (d) CeO_2-$NiCoO_x$@C and (e) $Co_{2-x}Ni_xP$@C.

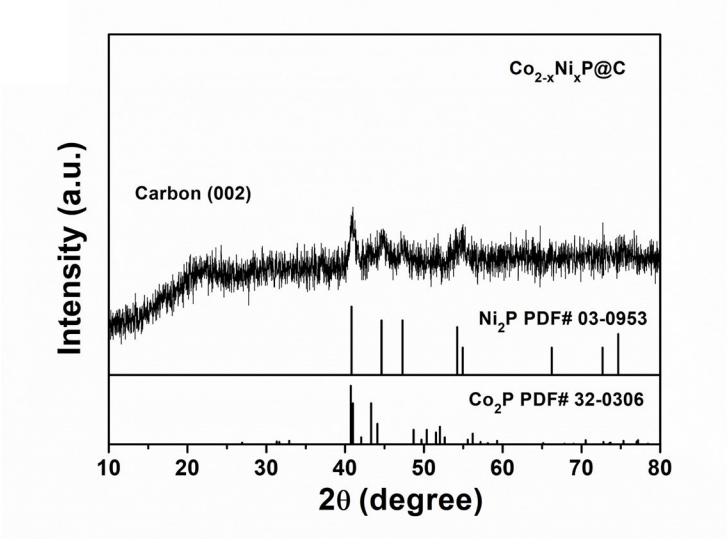

Figure S5. XRD pattern of the as-prepared $Co_{2-x}Ni_xP@C$.

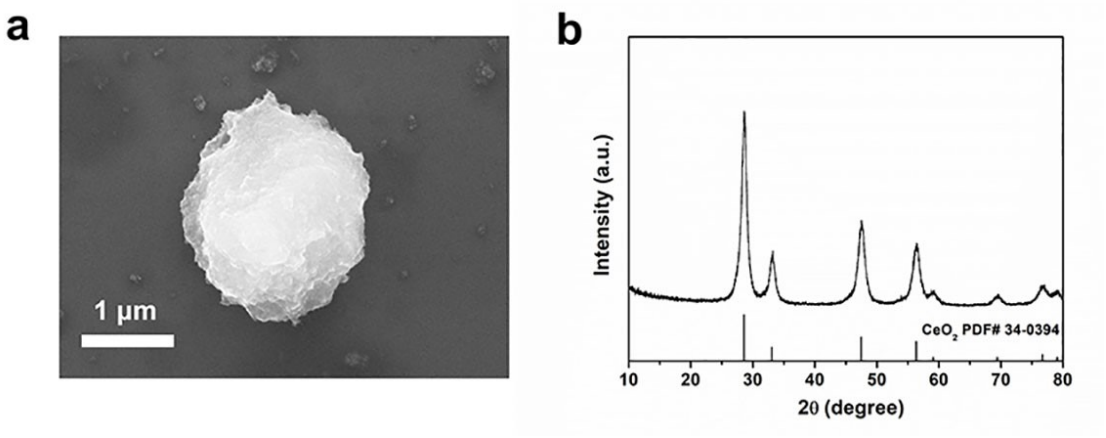

Figure S6. (a) SEM image and (b) XRD pattern of the as-prepared CeO_2.

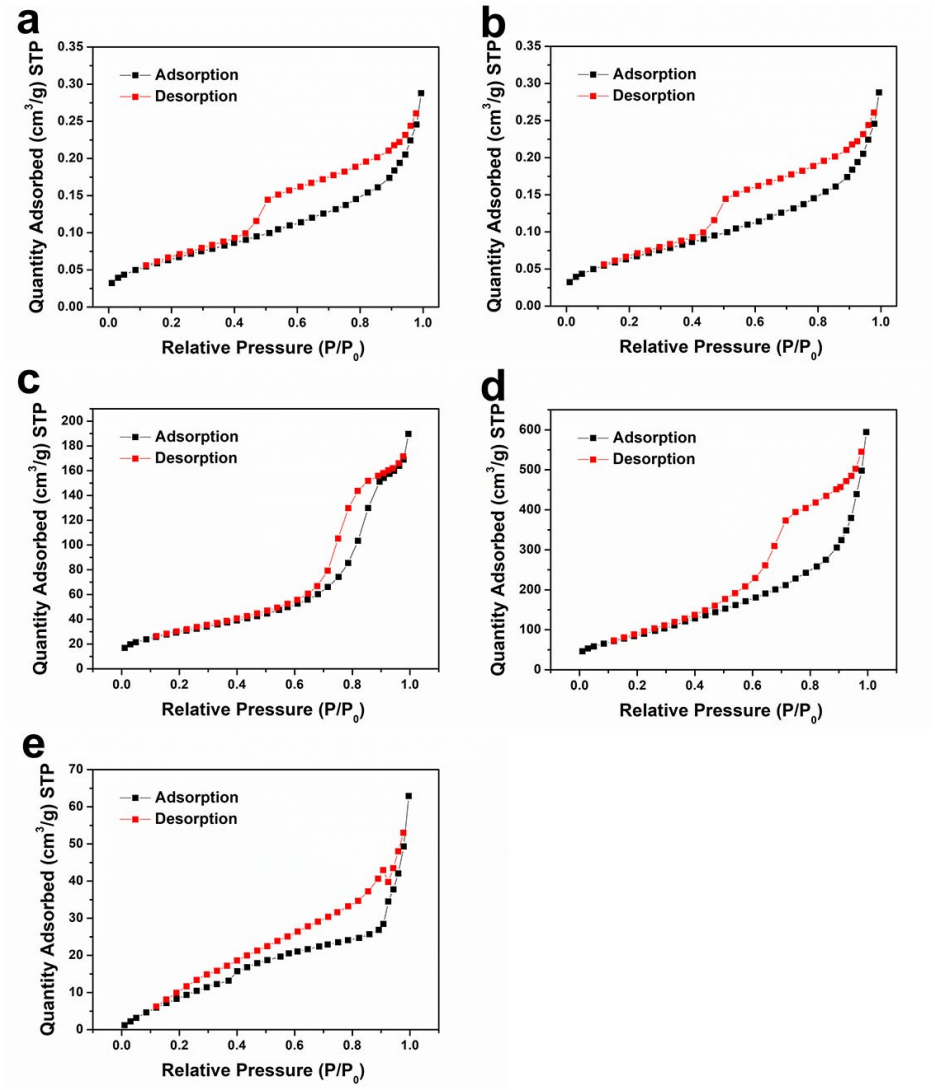

Figure S7. Nitrogen adsorption-desorption isotherms of the as-prepared (a) NiCo-MOF, (b) CeO_2-NiCo-MOF, (c) $Co_{2-x}Ni_xP$@C, (d) CeO_2-$Co_{2-x}Ni_xP$@C and (e) CeO_2.

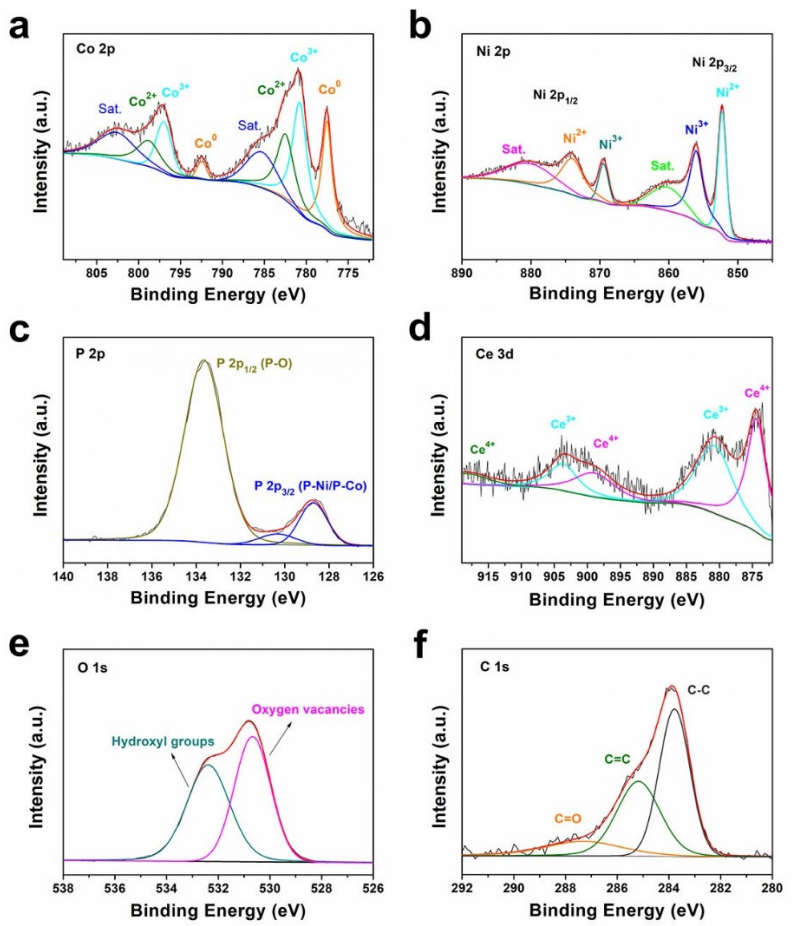

Figure S8. The high-resolution Co 2p (a), Ni 2p (b), P 2p (c), Ce 3d (d), O 1s (e) and C 1s (f) XPS spectra of the CeO_2-$Co_{2-x}Ni_xP$@C.

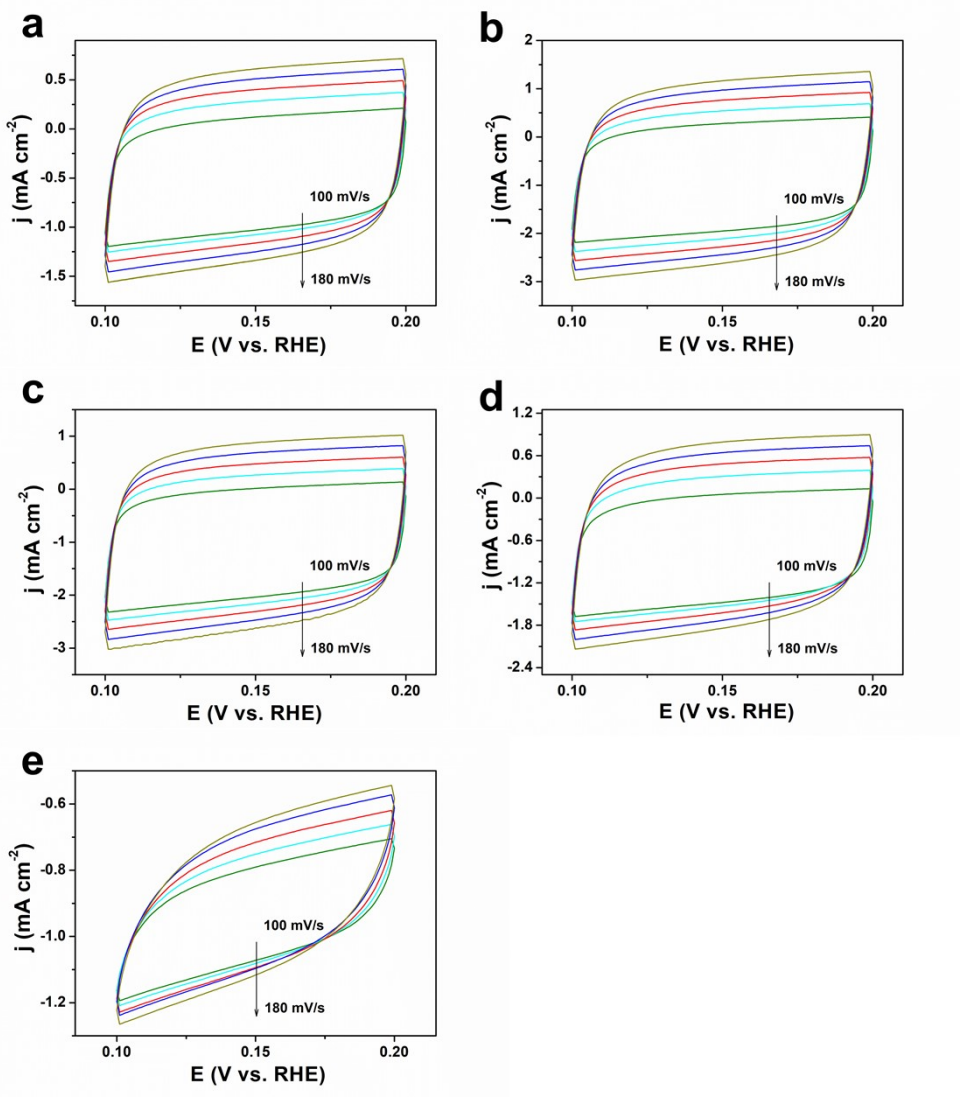

Figure S9. CV curves of (a) CeO_2-$Co_{2-x}Ni_xP$@C, (b) $Co_{2-x}Ni_xP$@C, (c) CeO_2-NiCo-MOF, (d) NiCo-MOF and (e) CeO_2 at 100-180 mV s^{-1} in the range of 0.1 and 0.2 V *vs.* RHE.

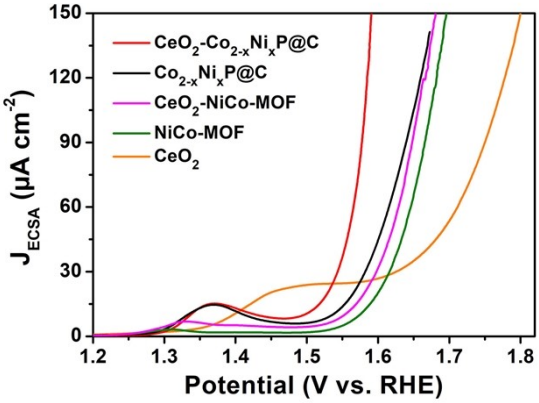

Figure S10. OER polarization curves normalized to the electrochemical active surface area (ECSA).

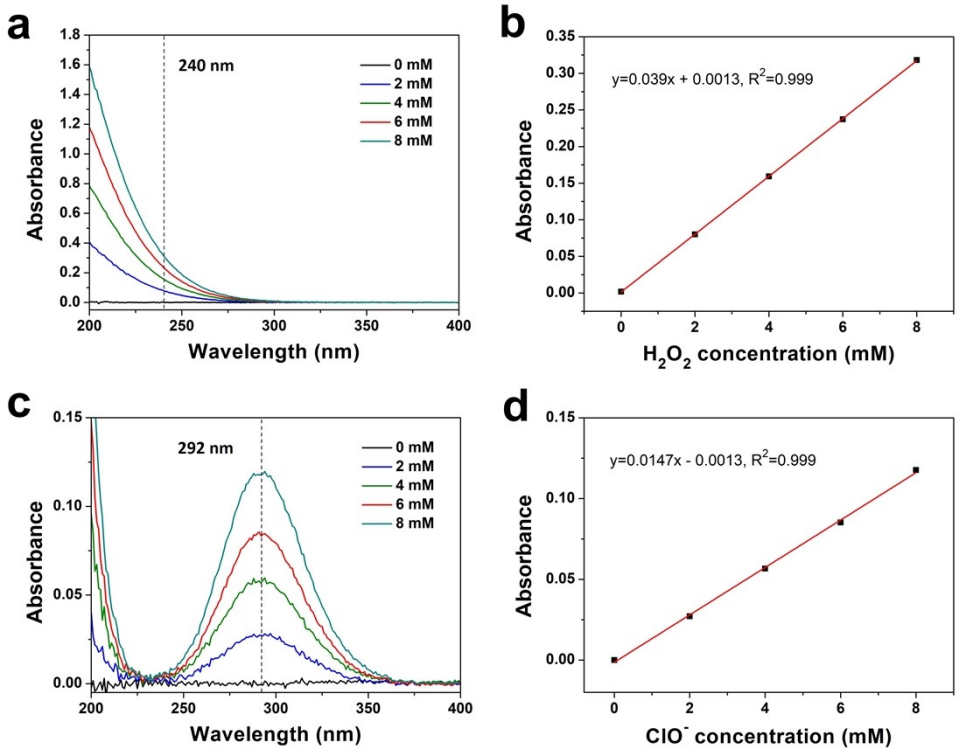

Figure S11. (**a**) UV-Vis absorption spectra of various H_2O_2 concentrations. (b) Calibration curve used for calculation of H_2O_2 concentrations. (**c**) UV-Vis absorption spectra of various ClO^- concentrations. (d) Calibration curve used for calculation of ClO^- concentrations.

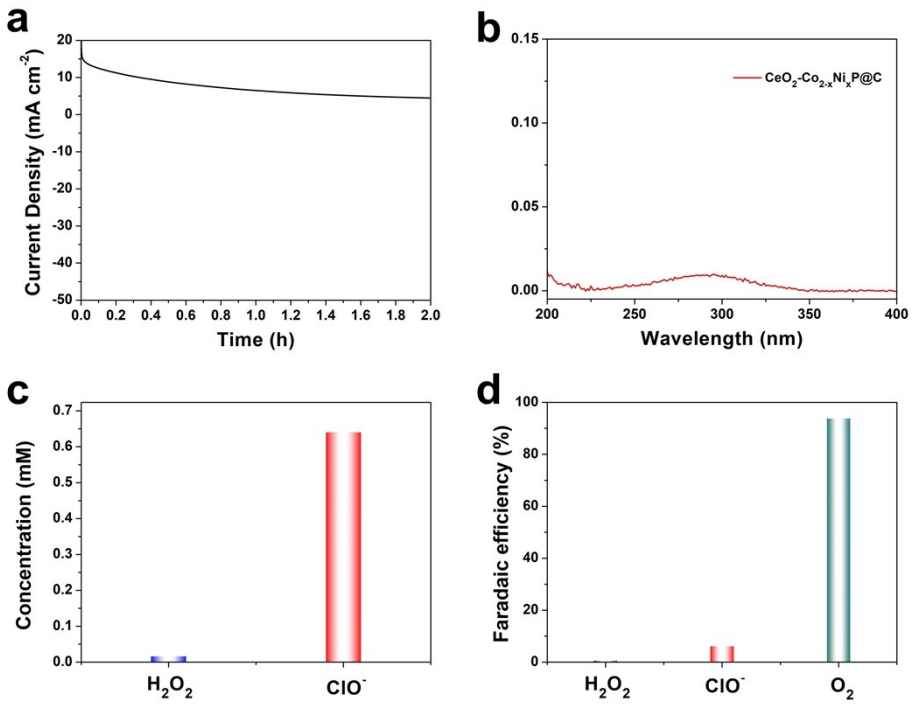

Figure S12. (**a**) Chronoamperometry curve of CeO_2-$Co_{2-x}Ni_xP$@C at 1.53 V *vs* RHE for 2 h in 1 M KOH + seawater. (b) UV-Vis absorption spectrum of 1 M KOH + seawater after 2 h electrolysis. (c) The calculated concentrations of H_2O_2 and ClO^-. (d) Faradaic efficiencies of OER and other two competing reactions.

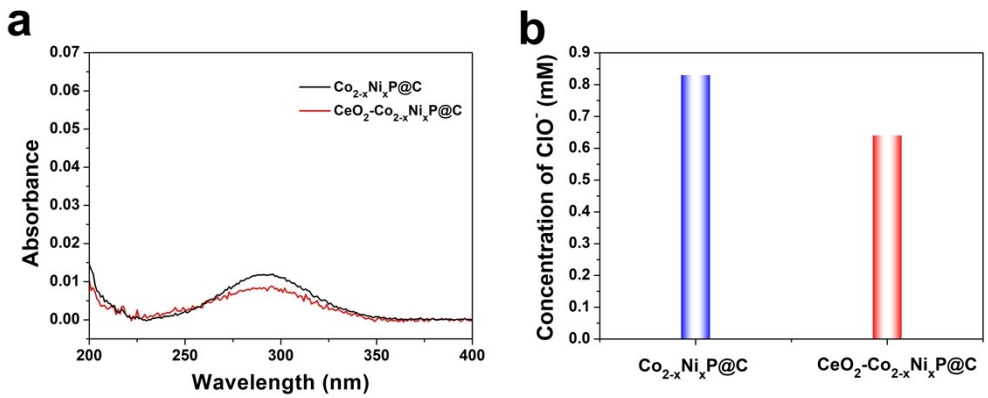

Figure S13. (**a**) UV-Vis absorption spectra of CeO_2-$Co_{2-x}Ni_xP$@C and $Co_{2-x}Ni_xP$@C after electrolysis 2 h at 1.53 V *vs* RHE for 2 h in 1 M KOH + seawater. (b) The corresponding calculated concentration of ClO^-.

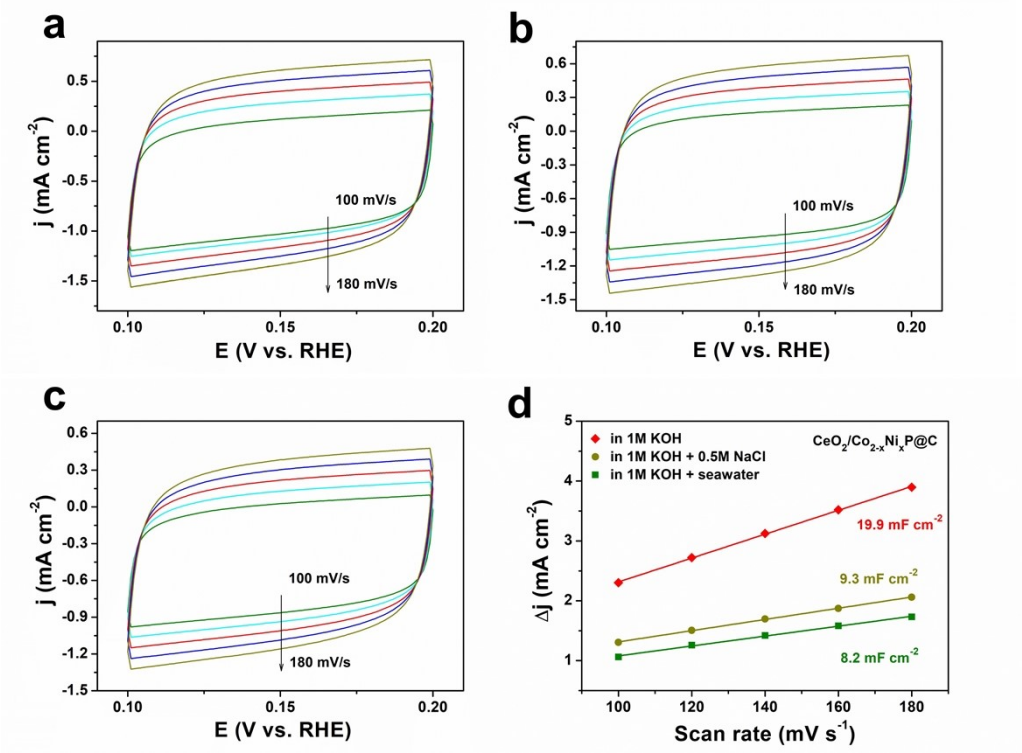

Figure S14. CV curves of CeO_2-$Co_{2-x}Ni_xP$@C in (a) 1 M KOH, (b) 1 M KOH + 0.5 M NaCl and (c) 1 M KOH + seawater. (d) Corresponding capacitive current densities at 0.15 V vs. RHE.

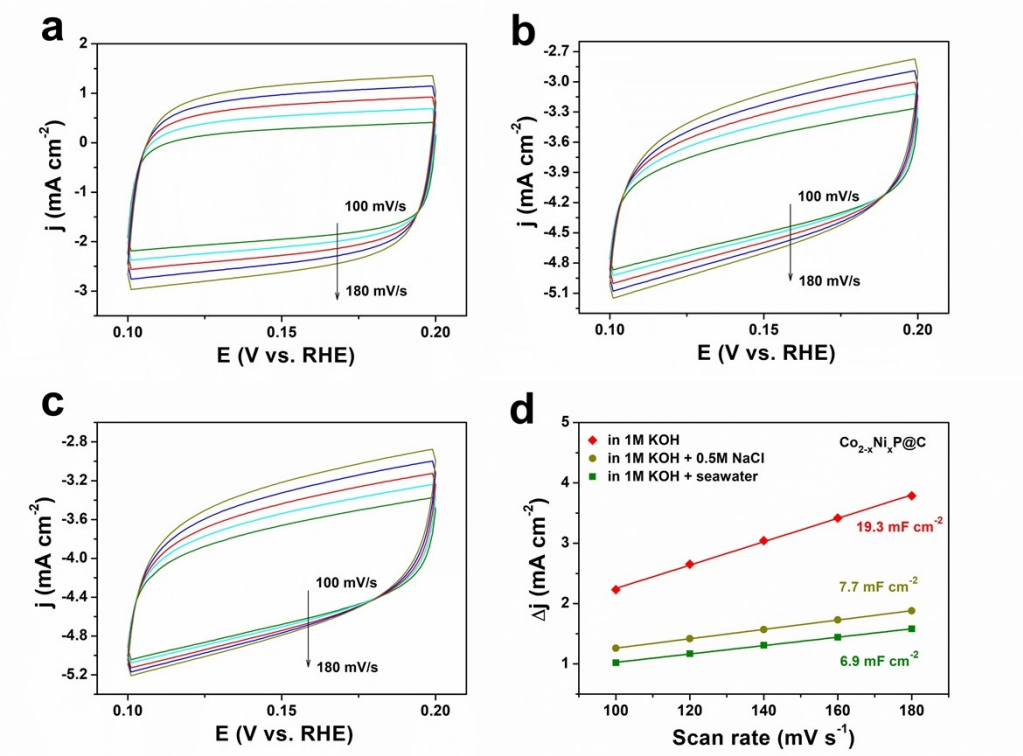

Figure S15. CV curves of $Co_{2-x}Ni_xP$@C in (a) 1 M KOH, (b) 1 M KOH + 0.5 M NaCl and (c) 1 M KOH + seawater. (d) Corresponding capacitive current densities at 0.15 V vs. RHE.

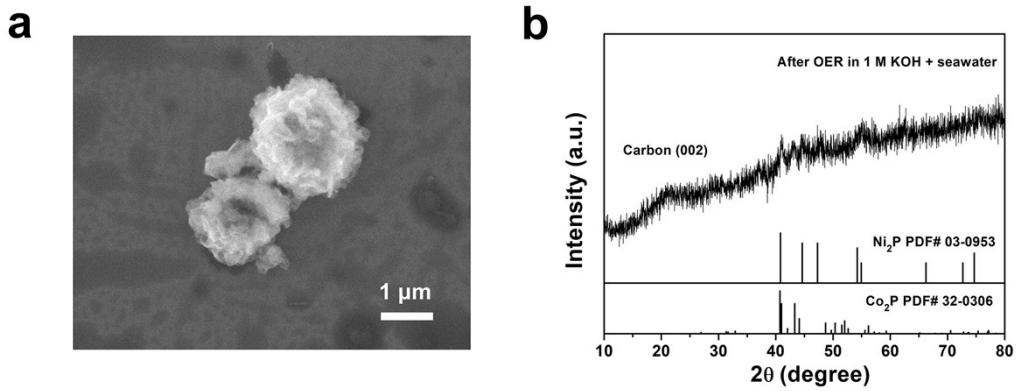

Figure S16. (a) SEM image and (b) XRD pattern of CeO_2-$Co_{2-x}Ni_xP$@C after 20 h stability test in 1 M KOH + seawater.

Table S1. Comparison of OER catalytic performance with other Ni and Co based electrocatalysts.

Catalyst	Electrolyte	η_{10} (mV)	Reference
CeO_2-$Co_{2-x}Ni_xP$@C	1M KOH	295	This work
Ni_2P−CoP	0.1M KOH	320	[1]
O–NiCoP Cages	1M KOH	310	[2]
Ni_3S_2-Co_9S_8/NCAs	1M KOH	337	[3]
CC@$NiCo_2O_4$	1M KOH	340	[4]
Zn-$NiCo_2O_4$	0.1M KOH	560	[5]
RuNi1Co1@CMT	1M KOH	299	[6]
RG/NCO NCs	6M KOH	313	[7]
NiO/CoN PINWs	1M KOH	300	[8]
CuNiCo oxide	1M KOH	312	[9]
Ni_2Co_2-CNR	0.1M KOH	310	[10]
C@NiCo	1M KOH	330	[11]
NCP@WPCA	1M KOH	351	[12]
Co0.25Ni0.75@NCNT	0.1M KOH	410	[13]
NiCo-$NiCoO_2$@Cu_2O@CF	1M KOH	327	[14]
$NiCo_2O_4$/NCNTs/NiCo	1M KOH	350	[15]

Table S2. Comparison of catalytic performance of different catalysts for seawater oxidation.

Catalyst	Electrolyte	η_{10} (mV)	Reference
CeO_2-$Co_{2-x}Ni_xP$@C	Seawater	320	This work
$Pb_2Ru_2O_{7-x}$	0.6M NaCl or NaClO4	500	[16]
Co-Fe LDH@Ti	Seawater	530	[17]
NiFe LDH	0.1 M KOH+0.5M NaCl	360	[18]
CaFeOx|FePO4@FTO	Phosphate buffered seawater	710	[19]
NiSx-CoSx	1M NaOH+1M NaCl	370	[20]
$Na_2Co_{1-x}Fe_xP_2O_7$@CC	0.1 M KOH+0.5 M NaCl	300	[21]
Co-N/C	Seawater	628	[22]
Co/Co_3O_4@C	Seawater	699	[23]

Supplementary references

1. X. Liang, B. Zheng, L. Chen, J. Zhang, Z. Zhuang and B. Chen, *ACS Appl. Mater. Interfaces,* 2017, **9**, 23222-23229.
2. D. Li, C. Zhou, Y. Xing, X. Shi, W. Ma, L. Li, D. Jiang and W. Shi, *Chem. Commun.*, 2021, **57**, 8158-8161.
3. X. Y. Wang, Y. Yang, R. Wang, L. Li, X. H. Zhao and W. M. Zhang, *Langmuir*, 2022, **38**, 7280-7289.
4. C. Guan, X. Liu, W. Ren, X. Li, C. Cheng and J. Wang, *Adv. Energy Mater.*, 2017, **7**, 1602391.
5. M. Yang, Y. Li, Y. Yu, X. Liu, Z. Shi and Y. Xing, *Chem.-Eur. J.,* 2018, **24**, 13002-13008.

6. Y. Xue, Q. Yan, X. Bai, Y. Xu, X. Zhang, Y. Li, K. Zhu, K. Ye, J. Yan, D. Cao and G. Wang, *J. Colloid Interface Sci.*, 2022, **612**, 710-721.
7. A. K. Samantara, S. Kamila, A. Ghosh and B. K. Jena, *Electrochim. Acta*, 2018, **263**, 147-157.
8. J. Yin, Y. Li, F. Lv, Q. Fan, Y.-Q. Zhao, Q. Zhang, W. Wang, F. Cheng, P. Xi and S. Guo, *ACS nano*, 2017, **11**, 2275-2283.
9. T. Priamushko, E. Budiyanto, N. Eshraghi, C. Weidenthaler, J. Kahr, M. Jahn, H. Tueysuez and F. Kleitz, *Chemsuschem*, 2022, **15**, e2021024.
10. W. Peng, J. Jin, S. Yang, Z. Shen, H. Wang, J. Zhang and G. Li, *ACS Appl. Energ. Mater.*, 2021, **4**, 11041-11050.
11. S. F. Tan, W. M. Ouyang, Y. J. Ji and Q. W. Hong, *J. Alloy. Compd.*, 2021, **889**, 161528.
12. C. Cui, X. X. Lai, R. H. Guo, E. H. Ren, W. F. Qin, L. Liu, M. Zhou and H. Y. Xiao, *Electrochim. Acta*, 2021, **393**, 139076.
13. A. Kundu, A. Samanta and C. R. Raj, *ACS Appl. Mater. Interfaces,* 2021, **13**, 30486-30496.
14. U. Y. Qazi, R. Javaid, M. Zahid, N. Tahir, A. Afzal and X. M. Lin, *Int. J. Hydrog. Energy*, 2021, **46**, 18936-18948.
15. C. Chen, H. Su, L. N. Lu, Y. S. Hong, Y. Z. Chen, K. Xiao, T. Ouyang, Y. L. Qin and Z. Q. Liu, *Chem. Eng. J.*, 2021, **408**, 127814.
16. P. Gayen, S. Saha and V. Ramani, *ACS Appl. Energ. Mater.*, 2020, **3**, 3978-3983.
17. F. Cheng, X. Feng, X. Chen, W. Lin, J. Rong and W. Yang, *Electrochim. Acta*, 2017, **251**, 336-343.
18. F. Dionigi, T. Reier, Z. Pawolek, M. Gliech and P. Strasser, *Chemsuschem*, 2016, **9**, 962-972.
19. W.-H. Huang and C.-Y. Lin, *Faraday Discuss.*, 2019, **215**, 205-215.
20. P. Hajjar, M.-A. Lacour, N. Masquelez, J. Cambedouzou, S. Tingry, D. Cornu and Y. Holade, *Molecules*, 2021, **26**, 5926.
21. H. J. Song, H. Yoon, B. Ju, D.-Y. Lee and D.-W. Kim, *Acs Catal.*, 2020, **10**, 702-709.

22. S. Kim, S. Ji, H. Yang, H. Son, H. Choi, J. Kang and O. L. Li, Appl. Catal. B-Environ., 2022, **310**, 121361.
23. Q. Zhang, X. Zhao, X. Miao, W. Yang, C. Wang and Q. Pan, *Int. J. Hydrog. Energy*, 2020, **45**, 33028-33036.
24. S. Cao, H. Huang, K. Shi, L. Wei, N. You, X. Fan, Z. Yang and W. Zhang, *Chem. Eng. J.,* 2021, **422**, 130123.
25. C. C. L. McCrory, S. Jung, I. M. Ferrer, S. M. Chatman, J. C. Peters, T. F. Jaramillo, *J. Am. Chem. Soc.* 2015, **137**, 4347-4357.